Batteries & Supercaps

Research Article
doi.org/10.1002/batt.202200285

Chemistry Europe
European Chemical Societies Publishing

www.batteries-supercaps.org

Fast Magnesium Conducting Electrospun Solid Polymer Electrolyte

Patrick Walke,[a, b] Janio Venturini,[a] Robert J. Spranger,[c] Leo van Wüllen,[c] and Tom Nilges*[a]

Magnesium Ion based Solid State Batteries (MIBs) are subject of intensive studies due to abundance of magnesium, its advantages in volumetric capacity, and the reduced dendrite growth. Here we report on a true solid polymer electrolyte system without liquid additives or plasticizers that reaches conductivities above 10^{-5} S cm^{-1} at room temperature and above 10^{-4} S cm^{-1} at 50 °C. An electrospun polymer electrolyte membrane fabricated from a polymer electrolyte featuring a composition of PEO:Mg(TFSI)$_2$ 36:1 [where PEO stands for poly(ethyleneoxide) and Mg(TFSI)$_2$ for magnesium bis(trifluoromethanesulfonyl) imide] was identified as the best performing system. Magnesium transport was substantiated by different methods, and the electrochemical properties including solid electrolyte interface (SEI) formation were investigated. Electrospinning as a preparation method has been identified as a powerful tool to enhance the electrochemical properties beyond conventional polymer membrane fabrication techniques.

Introduction

Since the development of lithium-ion batteries (LiB), which is inevitably connected to the names of Goodenough[1] and Yoshino[2] and the commercialization through Sony, the need to store large amounts of electrical energy has ever increased.[3] High-capacity batteries are indispensable not only for portable devices, but also to store energy produced from sustainable methods. Although the last decade has witnessed considerable progress in the development of new concepts such as lithium-air, lithium-sulfur or sodium-ion devices, batteries based on multivalent ions may evolve as a promising alternative.[4] The divalent Mg^{2+} ion, with its high abundance all over the globe[5] and its high specific gravimetric and volumetric capacities of 2300 mAh/g (Li 3862 mAh/g) and 3997 mAh/cm^3 (Li: 2062 mAh/cm^3),[3,6] respectively, holds considerable promise. In addition, the lower reducing character of Mg metal and its less-pronounced tendency to form dendrites (in contrast to pure Li) render Mg metal anodes more applicable with a variety of solvents and polymers.[7] Early electrolyte solutions with enhanced Mg dissolution und depleting abilities were based on *Grignard* reactions, before magnesium aluminate chloride complex solutions were intensively studied by the group of D. Aurbach.[3,8] Electrolyte solutions more similar to those used in LIBs are reported to show reasonable ionic conductivities and electrochemical behavior.[9] A full cell with Mg metal anode and $MgMn_2O_4$ cathode can be operated in a solution of 0.5 M $Mg(ClO_4)_2$ in acetonitrile acting as electrolyte.[10] Although it is reported that Mg(TFSI)$_2$ dissolved in ethers tends to form an insulating film on Mg metal anodes,[5b] a 1.0 M solution of Mg(TFSI)$_2$ in diglyme shows an ionic conductivity of 5×10^{-3} S cm^{-1} at r.t. with good Mg dissolution and deposition ability.[11] Besides liquid electrolytes, a variety of gel polymer electrolytes (GPEs) showed reasonably high conductivities.[12] A PVDF-HFP:Mg(O$_3$SCF$_3$)$_2$ with a molar ratio of 27:1 conducting-salt-containing polymer host enhanced by 40 w% 1-ethyl-3-methylimidazolium trifluoromethanesulfonate ionic liquid (EMITf) operating at r.t. reaches 4.63×10^{-3} S cm^{-1}.[13] To calculate the molarity of the statistical co-polymer, the average of the molar mass of the repeating units is used. By using 50 w% of EMITf on a poly(ethylene oxide) (PEO) based host with a molar composition of PEO:Mg(O$_3$SCF$_3$)$_2$ 25:1, an ionic conductivity of 5.6×10^{-4} S cm^{-1} is achieved at r.t., as compared to the same polymer: conducting salt host showing significantly lower ionic conductivity of 4×10^{-6} S cm^{-1} if no ionic liquid (IL) is added.[14] In addition to ILs, inorganic fillers can be added to enhance the electrochemical properties of solid polymer electrolytes (SPEs). An ionic conductivity of 1.6×10^{-4} S cm^{-1} at 30 °C is reported when 75 w% of 1-butyl-1-methylpyrrolidinium bis(trifluoromethyl)sulfonyl imide (Pyr_{14}-TFSI) ionic liquid and 10 w% TiO_2 are added to a PVDF-HFP:Mg(ClO$_4$)$_2$ host with a molar ratio of 5:8.[15] ILs are not the only compounds used as a liquid ingredient in GPEs. An ethylene carbonate/propylene carbonate (EC+PC) mixture admixed at a weight ratio of 5:1 to a polyacrylonitrile:Mg(O$_3$SCF$_3$)$_2$ 19:1 membrane reaches 1.7×10^{-4} S cm^{-1}.[16] The same carbonate combination is used to mobilize Mg ions in a poly(methyl methacrylate):Mg(O$_3$SCF$_3$)$_2$ host with a molar composition of 8:1. The resulting maximum ionic conductivity is reached at 3×

[a] Dr. P. Walke, Dr. J. Venturini, Prof. Dr. T. Nilges
Synthesis and Characterization of Innovative Materials, Chemistry Department
Technical University of Munich
Lichtenbergstraße 4, 85748 Garching bei München, Germany
E-mail: tom.nilges@tum.de
[b] Dr. P. Walke
TUMint.Energy Research GmbH
Lichtenbergstraße 4, 85748 Garching bei München, Germany
[c] R. J. Spranger, Prof. Dr. L. van Wüllen
Institute of Physics
University of Augsburg
Universitätsstraße 1, 86159 Augsburg, Germany

Supporting information for this article is available on the WWW under https://doi.org/10.1002/batt.202200285

Research Article
doi.org/10.1002/batt.202200285
Chemistry Europe
European Chemical Societies Publishing

10^{-4} S cm^{-1} with 300 w% EC + PC (liquid).[17] Instead of mixing short ether molecules, adding poly(ethylene glycol) dimethyl ether (PEGDE) was tried on an oligo(ethylene oxide)-crafted polymethacrylate (PEO-PMA) matrix. If an overall ratio of EO:MgX_2 of 128:1 is prepared the ionic conductivity ranges from 1×10^{-5} S cm^{-1} (X=O_3SCF_3), through 2×10^{-5} S cm^{-1} (X=ClO_4), to 1×10^{-4} S cm^{-1} (X=TFSI).[18] Because of the low molar mass of the used PEGDE (400–800 g mol^{-1}), this electrolyte is more related to GPEs than to SPEs, as stated by the authors. Although liquid electrolyte components are less of a safety issue in MIBs compared to LIBs due to the less reactive nature of the metal, the use of solid polymer electrolytes (SPEs) would introduce additional benefits such as reduced weight, toxicity, and risk of leaking. For a brief summary on inorganic MIB electrolytes, the interested reader is referred to a summary of Zhan et al.[19] A solvent-free example of SPEs is PVDF:$Mg(NO_3)_2$ 27:5, showing a poor ionic conductivity of 6×10^{-8} S cm^{-1} at r.t., which can be increased to 1.6×10^{-6} S cm^{-1} by adding 3 w% MgO.[20] As PEO is a well-known polymer to conduct alkali metals, several PEO:MgX_2 combinations without further additives have been tested. Most of these show low ionic conductivities ranging from 10^{-9} S cm^{-1} (X=ClO_4) to 10^{-7} S cm^{-1} (X=TFSI) at r.t.,[12] the latter at a molar composition of PEO:$Mg(TFSI)_2$ of 40:1.[21] This composition is close to the composition of choice in our study, as we use PEO:$Mg(TFSI)_2$ 36:1 as the highest processable Mg salt concentration for electrospun SPE membranes. Such conductivities are not competitive with state-of the art solid electrolytes and need to be improved prior to application. Target conductivities are in the range of 10^{-4} S cm^{-1}.[22]

In this contribution we present results on a novel $Mg(TFSI)_2$:PEO solid state electrolyte following an electrospinning synthesis route. In recent publications on Li and Na ion conducting SPEs with different AX (A=Li, Na; X=BF_4, TFSI), we showed that this synthesis route produces membranes with superior performance as compared to those prepared by more conventional approaches, i.e., solution casting or hot-pressing.[23] Whereas these produce bulk membranes, the electrospinning process yields membranes consisting of thin polymer fibers.[24]

As it is reported in literature that crystallinity in polymers hinders the ionic conductivity, we aimed for an amorphous phase as product. The outstanding properties of the products combined with the high grade of adaptability and the possibility of upscaling the electrospinning process to a roll-to-roll process make our electrospun polymer membrane a promising candidate to aim for lighter, safer, and more efficient battery systems in comparison to widely used Li-based batteries.[25]

Results and Discussion

Electrospinning is a powerful method to achieve large-area fibrous membranes with various additives and compositions. As illustrated and discussed earlier on for electrospun Na-PEO systems,[23c] the huge surface area of the fibrous material, in combination with an enhanced ion mobility and ion transport at the surface can be expected from electrospun systems.

By electrospinning solutions of PEO:$Mg(TFSI)_2$ with different molar compositions, amorphous membranes of submicrometric fibers are obtained. The fibers form homogenous membranes with up to 80 μm thickness. Figure 1 summarizes P-XRD experiments for various membranes where only few reflections were found. Reflections at 19.2 ° and 23.2 ° 2θ can be assigned to short range ordering of PEO chains.[26] No reflections indicating the presence of ordered $Mg(TFSI)_2$ are detected. The conductive salt does not influence the thickness or geometry of the fibers if the viscosity is controlled by the amount of solvent used. This is also true for the crystallinity as one cannot see any significant difference in number and intensity of reflections for the different samples.

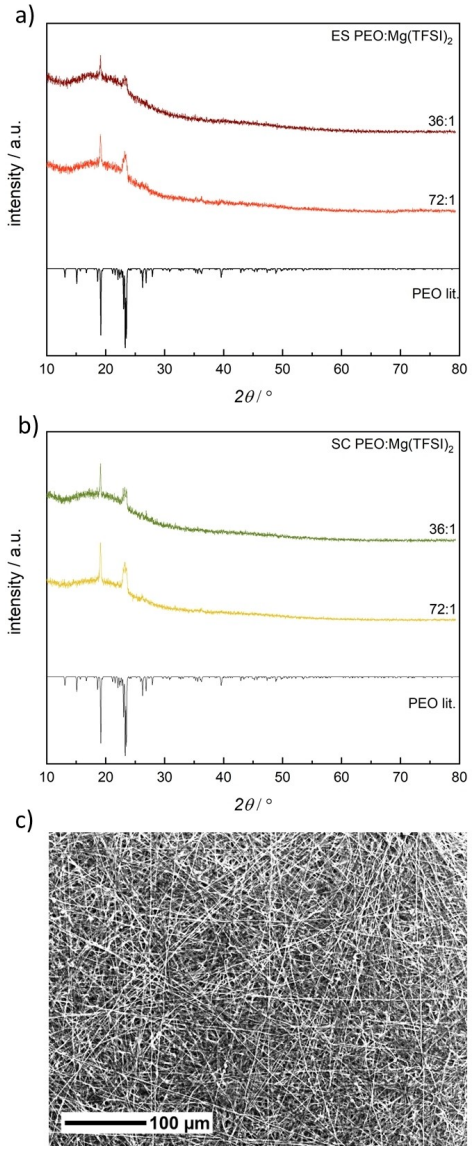

Figure 1. P-XRD of a) electrospun (ES) and b) solution casted (SC) PEO:$Mg(TFSI)_2$ SPEs with different molar compositions compared to a crystalline phase of PEO from literature.[34] Literature data are drawn with negative intensities. c) SEM image of an electrospun PEO:$Mg(TFSI)_2$ 36:1 SPE with 250-fold magnification.

Research Article
doi.org/10.1002/batt.202200285
Chemistry Europe
European Chemical Societies Publishing

The thermal properties of the membranes were studied by differential scanning calorimetry (DSC). The melting point decreases from 333 K to 322 K for electrospun PEO:$Mg(TFSI)_2$ 72:1 to 36:1. This trend is even more pronounced if the glass transition temperature is considered (257 K at 72:1, 234 K at 36:1), which is an interesting trend found by increasing the salt concentration (see Figure 2). In solution casted (SC) samples, T_g shows a non-uniform trend, increasing for the 36:1 (to 253 K) and decreasing (to 245 K) for the 72:1 system.

Ionic conductivities were determined by impedance spectroscopy. The ionic conductivity is dependent on the conducting salt concentration and the temperature. The electrospun sample with a molar composition of PEO:$Mg(TFSI)_2$ of 72:1 showed a conductivity of 6.0×10^{-8} S cm^{-1} at 273 K and 1.0×10^{-5} S cm^{-1} at 323 K. The highest ionic conductivity is achieved with a PEO:$Mg(TFSI)_2$ 36:1 SPE showing 1.8×10^{-6} S cm^{-1} at 273 K, which increases to 1.6×10^{-4} S cm^{-1} at 323 K, while a solution-casted sample of the same composition showed a drastically lower ionic conductivity, from 1.6×10^{-9} S cm^{-1} to 1.8×10^{-7} S cm^{-1} in the same temperature range (see Figure 3a). This again corroborates the superior performance of electrospun SPEs compared to solution casted SPEs, as already observed by us for related systems.[21] Consistently, the electrospun sample also showed the lowest glass transition temperature, which is directly linked to the mobility of PEO chains. All displayed ionic conductivities are calculated from the 4th cycle of temperature-dependent impedance spectroscopy to ensure a stable system during the measurement. The influence of the electrode material on the impedance spectroscopy results was checked by using stainless steel and Mg metal electrodes. While measuring with stainless steel blocking electrodes, the impedance showed the typical polarization at low frequencies; using Mg metal, a second semi-circle was detected at low frequencies in the Nyquist plot. This second semi-circle is assigned to the charge transfer from the Mg metal electrode to the SPE membrane (see S1, Supporting Information). With 20 consecutive impedance measurements at constant temperature (293 K) and voltage (0 V vs. OCV), the behavior of detected resistances was investigated. While the resistance at high frequencies – which is assigned to the conductivity along the fibers of the SPE – goes down by 13% due to compression of the sample, the interfacial resistance (surface contact resistances) goes up by 80% due to the formation of an electrolyte-electrode-interface (see S2, Supporting Information).

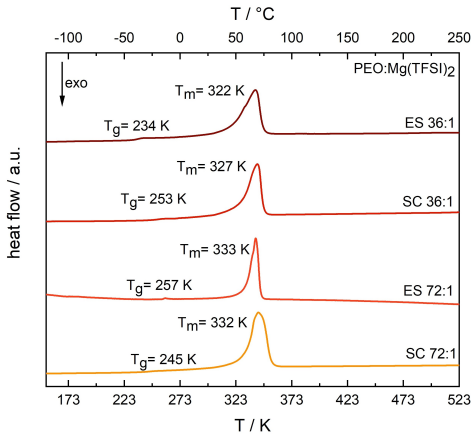

Figure 2. DSC curve of electrospun PEO:$Mg(TFSI)_2$ SPEs at different molar compositions and their fitted melting points T_m and glass transition temperatures T_g.

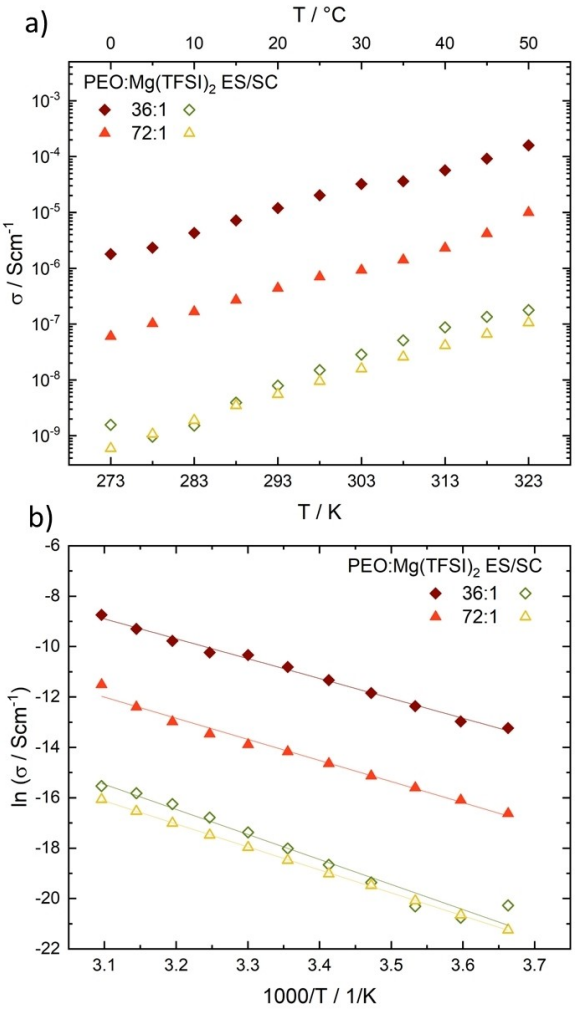

Figure 3. a) Ionic conductivity and b) Arrhenius type plots of electrospun (filled symbols) and solution-casted (empty symbols) SPEs with different compositions in a temperature range from 273 K to 323 K.

The activation energies as determined from the Arrhenius plots shown in Figure 3(b) are 66 kJ mol^{-1} for the 36:1 electrospun sample and 99 kJ mol^{-1} for a sample with lower salt concentration (72:1). Activation energies calculated for those membranes prepared via solution casting were determined to 49 kJ mol^{-1} to 82 kJ mol^{-1}, respectively (cf. Figure 3b).

For the sample with the highest ionic conductivity – an electrospun PEO:$Mg(TFSI)_2$ 36:1 membrane – neither NMR spectroscopy (see S4, Supporting Information) nor Karl-Fischer-titration indicated water contamination of the sample.

EDX spectroscopy was performed on a piece of the same membrane. The areal scan shows a homogenous distribution of Mg and F across the membrane. Besides Si coming from the used glassware, only C, O, F, Mg and S are detected. All these

Research Article
doi.org/10.1002/batt.202200285
Chemistry Europe
European Chemical Societies Publishing

elements can be assigned to the polymer or the $Mg(TFSI)_2$ conducting salt (see S3, Supporting Information).

The ability of PEO:$Mg(TFSI)_2$ SPEs to transport Mg ions through the membrane was proven by cyclic voltammetry on sample 36:1 between two Mg metal electrodes. The capacity dropped within the first 10–15 cycles, before reaching a plateau for at least 35 more cycles, as shown in Figure 4. Obviously, a passivation process at the SPE-electrode interface is initiated after the first cycles, causing a significant capacity loss during cycling. This is a widely known fact for Mg electrodes[27] which needs to be optimized in the future. However, the set of experiments at least substantiates the transport of Mg ions through the SPE.

Solid State NMR was employed to obtain more information about the dynamics of the salt and the PEO chains within the membrane. The results presented are obtained on the 36:1 sample synthesized via electrospinning.

To analyze the ion dynamic of the salt anion, TFSI, static temperature-dependent ^{19}F spectra were recorded, as shown in Figure 5(a). The ^{19}F signal is mainly dominated by the chemical shift and by dipole interactions, leading to the broadening of the signal. These internal interactions scale with the second Legendrian polynomial $3\cos^2(\beta) - 1$, with β representing the angle between the direction of the external magnetic field B_0 and directions of the principal axis of the respective interaction. Any motional process will lead to a total or partial averaging of these interactions, entailing a narrowing of the NMR line width (motional narrowing). As obvious from inspection of Figure 5(b), in which the observed ^{19}F static line width is plotted as a function of temperature, a drastic line narrowing of the ^{19}F static line width is observed starting at around 260 K, indicating the onset of dynamics at this temperature.

This temperature-dependent narrowing of the NMR line allows an estimation of the activation energy of the dynamic process of the TFSI-anion. According to the empirical Waugh-Fedin relation $E_A/\mathrm{kJmol^{-1}} = 0.156 \times T_{onset}/K$, the activation energy can be estimated.[28] The onset temperature here is the temperature at which the line width reduces to $(\upsilon_{\text{rigid lattice}} - \upsilon_{\text{motional narrowing}})/2 + \upsilon_{\text{motional narrowing}}$. From these parameters, an activation energy of 43 kJ/mol ($T_{onset} = 277$ K) was

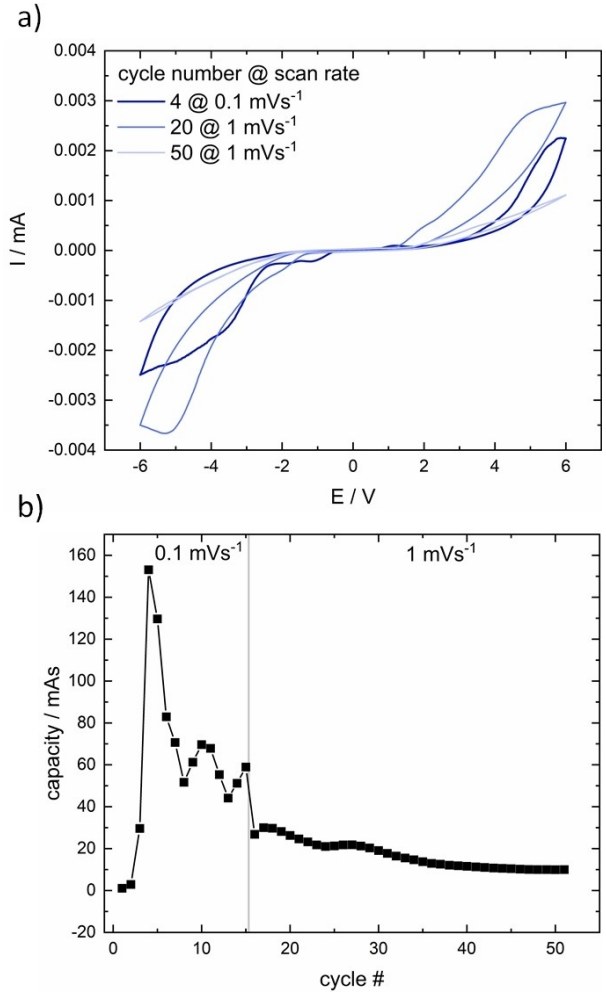

Figure 4. a) Single cycles of cyclic voltammetry at different scan rates of a PEO:$Mg(TFSI)_2$ 36:1 membrane between Mg metal electrodes in a coin cell. b) Capacity over cycle number calculated from CV cycling, scan rates given in the graph.

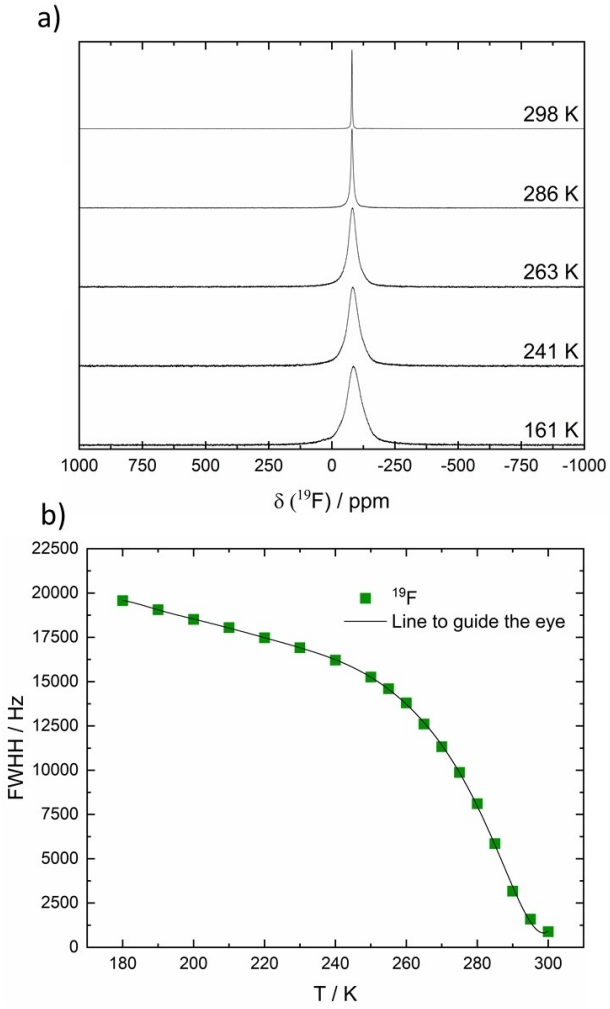

Figure 5. a) Temperature-dependent static ^{19}F spectra and b) the evolution of the ^{19}F line width as a function of temperature for the PEO:$Mg(TFSI)_2$ 36:1 membrane. The line is just a guide to the eye.

Research Article
doi.org/10.1002/batt.202200285
Chemistry Europe
European Chemical Societies Publishing

determined. The calculated activation energy of the $Mg(TFSI)_2$-based plasticizer-free sample is comparable to the LiTFSI plasticizer-free sample with an activation energy of 41 kJ/mol for a PEO:LiTFSI 18:1 membrane.[23a]

We studied the dynamics of the PEO chains within the membrane via ^{13}C-NMR. With temperature dependent ^{13}C-MAS single pulse and ^{13}C-{^1H}-CP-MAS experiments, it is possible to focus on those ^{13}C nuclei within mobile PEO species (single pulse) or immobile PEO species (^{13}C CPMAS).

Since the resonances of ^{13}C in immobile PEO are broadened beyond detectability due to the strong heteronuclear decoupling in a single pulse excitation ^{13}C-MAS NMR experiment, this experiment highlights ^{13}C nuclei in mobile environments. On the other hand, the ^{13}C-{^1H}-CPMAS experiment focuses on ^{13}C nuclei embedded in immobile environments, since the efficiency of the cross-polarization process relies on the heteronuclear dipolar coupling between ^{13}C and ^1H.

Thus, the results presented in Figure 6 clearly show the onset of PEO chain mobility at temperatures around r.t. Whereas the CPMAS signal (highlighting the immobile PEO species) at low temperatures exhibits a set of individual lines which can be assigned to crystalline PEO (narrow signals in the range from 70 to 74 ppm) and an amorphous PEO:salt complex (broad signal at 69 ppm),[29] the overall signal intensity increases with increasing temperatures and the lines smear into a single signal, which is lost at around r.t. On the other hand, the single pulse ^{13}C MAS signal is absent until 290 K and first observed at 303 K. The signal shape indicates the presence of a triplet which arises due to the *J*(C–H) coupling with the methylene protons. The intensity of this triplet increases with increasing temperatures. In addition, two narrow signals occur at 117.9 ppm and 122.4 ppm. These signals can be assigned to the inner two lines of a quartet due to the J(C–F) coupling of the CF_3 groups of the TFSI anion. The detectability of the triplet indicates the complete removal of the strong heteronuclear dipolar coupling (^{13}C ^1H) and thus indicates a rather vivid PEO chain dynamics. However, as compared to the monovalent systems PEO:$LiBF_4$ and PEO:LiTFSI, both fabricated via electrospinning, the onset of this motional process is shifted to somewhat higher temperatures.[23a,30] This may indicate a stronger

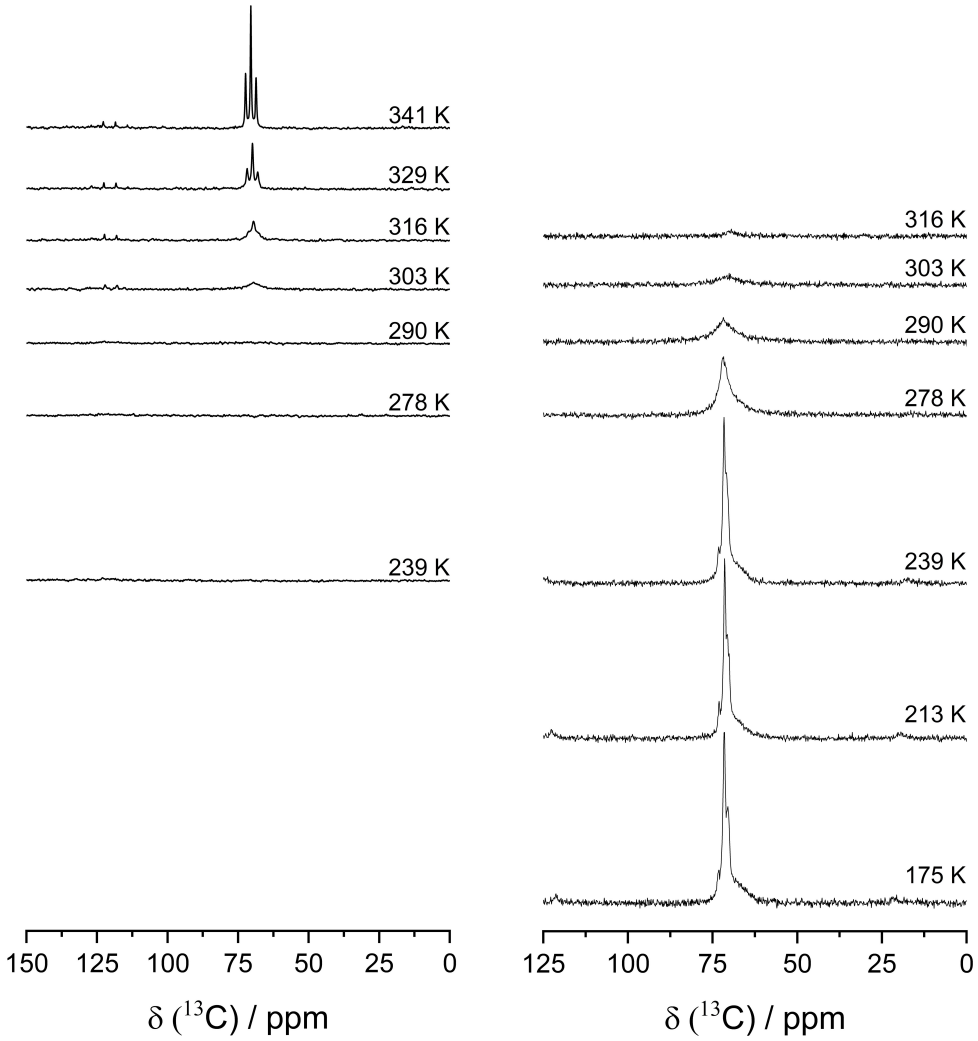

Figure 6. Temperature-dependent ^{13}C-MAS spectra (left) and ^{13}C-{^1H}-CP-MAS spectra (right) for the PEO:$Mg(TFSI)_2$ 36:1 membrane for the indicated temperatures.

coordination of the divalent Mg^{2+} cation to the ether oxygen atoms.

Conclusion

Our electrospun PEO-based solid polymer electrolyte PEO:Mg(TFSI)$_2$ 36:1 shows an ionic conductivity of 2.0×10^{-5} S cm^{-1} at r.t. without the use of any liquid, organic, or inorganic additive. The ionic conductivity of the electrospun samples proves to be higher compared to the samples prepared via solution casting and at least one order of magnitude higher than those SPEs reported in literature, while the concentration of the Mg^{2+} ions is lower than in most of them, cf. Figure 7. By using electrochemical and analytical methods, we showed that PEO:Mg(TFSI)$_2$ SPEs with different molar compositions can successfully be prepared by electrospinning and solution casting. The electrospun PEO:Mg(TFSI)$_2$ 36:1 membrane shows the highest ionic conductivity over the complete measured temperature range from 273 K to 323 K, the melting temperature of the system. The analysis of the thermal behavior led to the conclusion that a membrane at a molar composition of PEO:Mg(TFSI)$_2$ 36:1 has a lowered glass transition temperature. Solid State NMR attests the absence of any impurities or side phases other than the PEO:Mg(TFSI)$_2$ electrolyte and proves anion and PEO segmental mobility commencing at temperatures around r.t. As the membranes are free of water and other solvents, the determined conductivity has to be ascribed to the Mg^{2+} and $TFSI^-$ ions in the SPE. The conducted cyclic voltammetry and impedance spectroscopy in symmetrical Mg metal cells also clarify that the Mg^{2+} ions contribute to the ionic conductivity, as Mg metal electrodes function as blocking electrodes to every species other than Mg^{2+} ions. The current in the cyclic voltammetry is low due to the known problem of an electrode-SPE-interface resistance formation due to passivation processes. This interfacial resistance is determined via impedance spectroscopy. It rises with time to a plateau, illustrating that a passivation process occurs on the Mg-electrode. Although metallic Mg is known to be less reactive compared to lithium or sodium, this indicates that the reactivity is still high enough to build up an interface layer when in contact with the SPE, albeit not affecting the high ion mobility

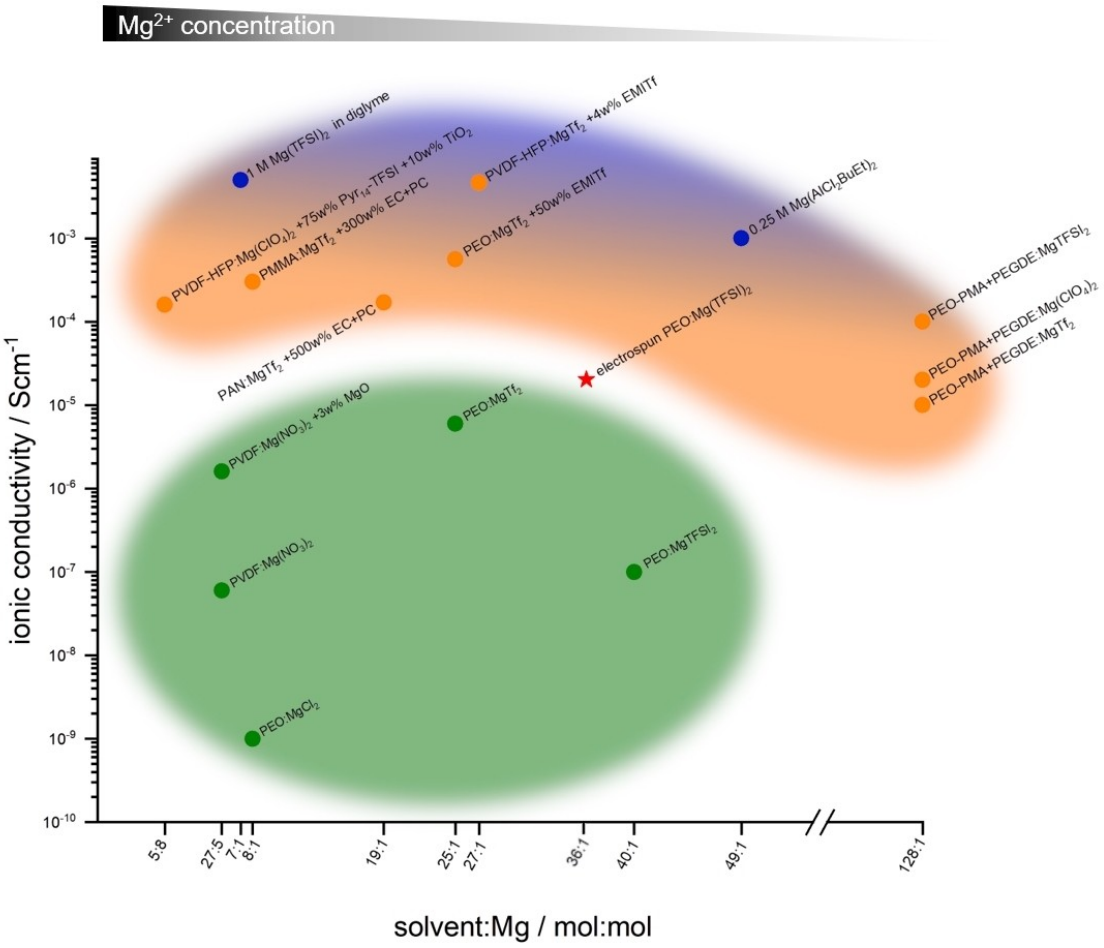

Figure 7. Room temperature ionic conductivity of solid polymer electrolytes (green), gel polymer electrolytes (orange) and two examples of liquid electrolytes (blue) sorted by their Mg^{2+} concentration. Red star marks the electrospun PEO:Mg(TFSI)$_2$ 36:1 membrane, which is the best performing pure, (ionic) liquid-free, solid electrolyte in this work.[10,11,14–21,23,24]

Research Article
doi.org/10.1002/batt.202200285
Chemistry Europe
European Chemical Societies Publishing

in the electrolyte. All these results lead to the conclusion that the electrospun PEO:$Mg(TFSI)_2$ 36:1 SPE is an Mg ion conductor with 1000× higher conductivity compared to the PEO:$Mg(TFSI)_2$ SPEs with similar molar composition reported in literature. A model to describe and explain the enhanced performance of electrospun Li- and Na-PEO systems which incorporates an enlarged surface area and enhanced ion mobility at the surface of the fibers seems also to be valid for Mg-PEO systems. Together with the demonstrated increase in conductivity when switching from solution casting to electrospinning, this work emphasizes potential of Mg ion electrolytes and the positive effect of electrospinning to the field.

Experimental

Preparation of membranes

Molar compositions of the SPEs PEO:$Mg(TFSI)_2$ are given throughout the text as X:1, with X denoting the relative molar amount of PEO compared to that of $Mg(TFSI)_2$. Two different compositions were investigated in this work, 36:1 and 72:1, and both were prepared via electrospinning and solution casting. The electrospinning solution was prepared by dissolving PEO (M_W = 300,000 g/mol, Sigma Aldrich) in acetonitrile (>99%, Sigma Aldrich). After the polymer was fully dissolved, $Mg(TFSI)_2$ (>99%, Sigma Aldrich) was added in a specific molar ratio (see Table 1). Since it is known that the addition of succinonitrile (SN) as a solid lubricant induces a drastic enhancement of the polymer dynamics and hence entails in increased ionic conductivity[30] we attempted to include SN into the membranes. However, it turned out that this was not successful since the NMR results reveal that only a small fraction of SN was incorporated into the membranes.

Fibrous membranes were manufactured in a homemade electrospinning apparatus, as described elsewhere.[23b] All PEO:$Mg(TFSI)_2$ solid polymer electrolytes were obtained by passing the prepared solution through a capillary (0.9 mm inner diameter) with a flow rate of 2–3 mL/h. A voltage of 17–20 kV was applied at the capillary. The fibers were collected on a grounded ring collector (10 cm diameter). The obtained dense fiber network was dried for 24 h at 10^{-3} mbar at r.t. and stored under inert atmosphere in a glovebox (mBraun, $H_2O < 0.1$ ppm, $O_2 < 0.1$ ppm) before being submitted to characterization methods. The solution casted samples were prepared by casting the prepared solutions on glass and drying them at 10^{-2} mbar at r.t. for 24 h.

X-ray powder diffraction phases analysis

Powder XRD measurements of selected membranes were executed on a STOE STADI–P diffractometer (Cu–Kα_1 radiation, λ = 1.54051 Å, Ge monochromator) with a flat-bed sample holder. α-Si (a = 5.43096 Å) was used as internal standard. The sample membranes were punched out from the already-prepared and dried membranes and measured directly in transmission geometry.

Table 1. Molar composition of polymer membranes and the used amount of reagents.

PEO:$Mg(TFSI)_2$	PEO	$Mg(TFSI)_2$	acetonitrile
36:1	0.3500 g	0.1291 g	5.5 mL
72:1	0.3500 g	0.0645 g	6 mL

Differential scanning calorimetry

Thermal properties of selected membranes were examined by Differential Scanning Calorimetry (DSC) in Al-crucibles using a DSC 200 calorimeter F3 Maia by Netzsch. The crucibles were closed inside a Glovebox ($H_2O < 0.1$ ppm, $O_2 < 0.1$ ppm). The measurements are conducted in a temperature range from 123 K to 523 K with a heating rate of 10 K/min. Only the first heating cycle is used for comparison.

Potentiostatic electrochemical impedance spectroscopy

To evaluate the ionic conductivity, disks of 10 mm diameter were placed between two stainless steel electrodes (8 mm diameter) in a TSC battery cell (rhd instruments). During the measurement a pressure of 3.4 bar was applied to the sample. The cell was placed in a temperature-controlled cell stand (Microcell HC, rhd instruments) and connected to a potentiostat (Metrohm Autolab B.V. Typ PGSTAT204). Impedance spectroscopy was performed in a frequency range from 10 MHz to 10 Hz with an amplitude of 20 mV. The temperature was varied for four cycles from 273 K to 323 K in 5 K steps. Each temperature was held constant for 20 min before the electrochemical measurement was started, to ensure a uniform temperature across the sample. The thickness of the membranes was measured using a micrometer screw (Holex, 0–25 mm) with 0.001 mm accuracy. The ionic conductivity σ was calculated from the high frequency resistance (R) of the equivalent circuit with the following relation:

$$\sigma = \frac{d}{R \times A} \tag{1}$$

where d and A are the thickness and cross-section area of the samples, respectively. The activation energy was obtained from the Arrhenius equation:

$$\sigma = B \bullet exp(-E_a/RT) \tag{2}$$

where B, E_a, R, and T are pre-exponential factor, activation energy, gas constant, and temperature, respectively.

Cyclic voltammetry

Electrochemical cycling was performed in symmetric cells using 2032-type coin cells. Therefore, 17 mm disks of the samples were placed between Mg metal electrodes (0.5 mm thickness, 14 mm diameter, 99%, Sigma Aldrich). Cycling voltammetry was carried out from −6 V to 6 V with a scan rate of 0.1 mV/s at 298 K using a Biologic VMP3 potentiostat.

Karl Fischer titration

To conduct conventional Karl-Fischer-Titration, a piece (30 mg) of the electrospun membrane is dissolved in pre-dried (< 1.0 ppm H_2O) acetonitrile (1 mL).

NMR spectroscopy

For the solid state nuclear magnetic resonance experiments a BRUKER Avance III spectrometer in combination with a 7 T magnet was used. The experiments were performed at resonance frequencies of 75.5 MHz, 282.5 MHz and 300.2 MHz for ^{13}C, ^{19}F and ^{1}H respectively. To reference the NMR-spectra, $CFCl_3$(aq.) and Adaman-

tane were used for ^{19}F, ^{13}C, and ^{1}H, respectively. For the measurements a 4 mm triple resonance and a 4 mm double resonance probe were used. To obtain information about the dynamic processes of the TFSI anion, static temperature-dependent ^{19}F measurements were performed. For the temperature calibration, static ^{207}Pb NMR measurements of $Pb(NO_3)_2$ were performed, using the temperature dependence of the chemical shift of ^{207}Pb as a chemical shift thermometer.[31] In addition ^{13}C-MAS experiments were performed to investigate the PEO host structure of the membrane.

The repetition delays for the ^{19}F single pulse experiments were set to 5 s; for the ^{13}C single pulse experiments and ^{13}C-{^{1}H}-CP-MAS relation delays of 10–30 s and 10 s, respectively, were used. The contact time in the CPMAS experiments was set to 0.5 ms.

^{25}Mg NMR could offer a direct tool to assess Mg mobility within the studied electrolytes. However, the rather low gyromagnetic ratio (-1.639×10^{7} rads^{-1}T^{-1}) necessitates specialized probes not available in our laboratory.

Scanning electron microscopy and energy-dispersive X-ray spectroscopy

To observe the fibrous structure of the prepared membranes, small samples of the dried SPEs are fixed to a conductive carbon tape and attached to the sample holder of the scanning electron microscope (SEM). As energy-dispersive X-ray spectroscopy (EDX) is required, the sample holder is transferred to the vacuum chamber of a JOEL JCM-6000 NeoScop™, which is operated with a JEOL JED-2200 EDS. For SEM imaging an acceleration of 15 kV is applied.

Supporting Information

Nyquist-Plots of cells with blocking or Mg metal electrodes and during cell aging, SEM and EDX images, NMR spectra

Funding Sources

This work was founded by the DFG under grants Ni1095/9-1 and WU237/9-1 and is part of the project "Industrialisierbarkeit von Festkörperelektrolytzellen" funded by the Bavarian Ministry of Economic Affairs, Regional Development and Energy. Open Access funding enabled and organized by Projekt DEAL.

Conflict of Interest

The authors declare no conflict of interest.

Data availability Statement

The data that support the findings of this study are available from the corresponding author upon reasonable request.

Keywords: solid polymer electrolyte · magnesium battery · electrospinning · impedance spectroscopy · ionic conductivity

[1] K. Mizushima, P. C. Jones, P. J. Wiseman, J. B. Goodenough, *Solid State Ionics* **1981**, *3–4*, 171–174.
[2] A. Yoshino, *Angew. Chem. Int. Ed.* **2012**, *51*, 5798–5800; *Angew. Chem.* **2012**, *124*, 5898–5900.
[3] R. Attias, M. Salama, B. Hirsch, Y. Goffer, D. Aurbach, *Joule* **2019**, *3*, 27–52.
[4] a) A. Ponrouch, J. Bitenc, R. Dominko, N. Lindahl, P. Johansson, M. R. Palacin, *Energy Storage Mater.* **2019**, *20*, 253–262; b) R. C. Massé, E. Uchaker, G. Cao, *Sci. China Mater.* **2015**, *58*, 715–766.
[5] a) C. Xu, Y. Chen, S. Shi, J. Li, F. Kang, D. Su, *Sci. Rep.* **2015**, *5*, 14120; b) L. P. Lossius, F. Emmenegger, *Electrochim. Acta* **1996**, *41*, 445–447.
[6] J. Song, E. Sahadeo, M. Noked, S. B. Lee, *J. Phys. Chem. Lett.* **2016**, *7*, 1736–1749.
[7] a) M. Jäckle, A. Groß, *J. Chem. Phys.* **2014**, *141*, 174710; b) R. Davidson, A. Verma, D. Santos, F. Hao, C. Fincher, S. Xiang, J. Van Buskirk, K. Xie, M. Pharr, P. P. Mukherjee, S. Banerjee, *ACS Energy Lett.* **2019**, *4*, 375–376.
[8] a) D. Aurbach, Z. Lu, A. Schechter, Y. Gofer, H. Gizbar, R. Turgeman, Y. Cohen, M. Moshkovich, E. Levi, *Nature* **2000**, *407*, 724–727; b) Y. Gofer, O. Chusid, H. Gizbar, Y. Viestfrid, H. E. Gottlieb, V. Marks, D. Aurbach, *Electrochem. Solid-State Lett.* **2006**, *9*, A257.
[9] Z. Ma, D. R. MacFarlane, M. Kar, *Batteries & Supercaps* **2019**, *2*, 115–127.
[10] Q. D. Truong, M. Kempaiah Devaraju, P. D. Tran, Y. Gambe, K. Nayuki, Y. Sasaki, I. Honma, *Chem. Mater.* **2017**, *29*, 6245–6251.
[11] N. Sa, N. N. Rajput, H. Wang, B. Key, M. Ferrandon, V. Srinivasan, K. A. Persson, A. K. Burrell, J. T. Vaughey, *RSC Adv.* **2016**, *6*, 113663–113670.
[12] B. Park, J. L. Schaefer, *J. Electrochem. Soc.* **2020**, *167*, 070545.
[13] X. Tang, R. Muchakayala, S. Song, Z. Zhang, A. R. Polu, *J. Ind. Eng. Chem.* **2016**, *37*, 67–74.
[14] Y. Kumar, S. A. Hashmi, G. P. Pandey, *Electrochim. Acta* **2011**, *56*, 3864–3873.
[15] R. Deivanayagam, M. Cheng, M. Wang, V. Vasudevan, T. Foroozan, N. V. Medhekar, R. Shahbazian-Yassar, *ACS Appl. Energ. Mater.* **2019**, *2*, 7980–7990.
[16] G. G. Kumar, N. Munichandraiah, *Solid State Ionics* **2000**, *128*, 203–210.
[17] G. Girish Kumar, N. Munichandraiah, *Electrochim. Acta* **2002**, *47*, 1013–1022.
[18] M. Morita, N. Yoshimoto, S. Yakushiji, M. Ishikawa, *Electrochem. Solid-State Lett.* **2001**, *4*, A177.
[19] Y. Zhan, W. Zhang, B. Lei, H. Liu, W. Li, *Front. Chem.* **2020**, *8*, 125.
[20] Nidhi, S. Patel, R. Kumar, *J. Alloys Compd.* **2019**, *789*, 6–14.
[21] A. Bakker, S. Gejji, J. Lindgren, K. Hermansson, M. M. Probst, *Polymer* **1995**, *36*, 4371–4378.
[22] J. C. Bachman, S. Muy, A. Grimaud, H.-H. Chang, N. Pour, S. F. Lux, O. Paschos, F. Maglia, S. Lupart, P. Lamp, L. Giordano, Y. Shao-Horn, *Chem. Rev.* **2016**, *116*, 140–162.
[23] a) P. Walke, K. M. Freitag, H. Kirchhain, M. Kaiser, L. van Wüllen, T. Nilges, *Z. Anorg. Allg. Chem.* **2018**, *644*, 1863–1874; b) K. M. Freitag, H. Kirchhain, L. van Wüllen, T. Nilges, *Inorg. Chem.* **2017**, *56*, 2100–2107; c) K. M. Freitag, P. Walke, T. Nilges, H. Kirchhain, R. J. Spranger, L. van Wüllen, *J. Power Sources* **2018**, *378*, 610–617.
[24] S. N. Banitaba, D. Semnani, M. Karimi, E. Heydari-Soureshjani, B. Rezaei, A. A. Ensafi, *Electrochim. Acta* **2021**, *368*, 137339.
[25] a) L. Persano, A. Camposeo, C. Tekmen, D. Pisignano, *Macromol. Mater. Eng.* **2013**, *298*, 504–520; b) W. E. Teo, S. Ramakrishna, *Nanotechnology* **2006**, *17*, R89-R106.
[26] Y. Takahashi, I. Sumita, H. Tadokoro, *J. Polym. Sci. Polym. Phys. Ed.* **1973**, *11*, 2113–2122.
[27] B. Li, R. Masse, C. Liu, Y. Hu, W. Li, G. Zhang, G. Cao, *Energy Storage Mater.* **2019**, *22*, 96–104.
[28] J. Waugh, E. I. Fedin, *Soviet Physics-Solid State* **1963**, *4*, 1633–1636.
[29] H. Kirchhain, Dissertation thesis, (Augsburg), **2020**.
[30] N. Voigt, L. van Wüllen, *Solid State Ionics* **2014**, *260*, 65–75.
[31] A. Bielecki, D. P. Burum, *J. Magn. Reson. Ser. A* **1995**, *116*, 215–220.

Manuscript received: June 24, 2022
Revised manuscript received: October 10, 2022
Accepted manuscript online: October 11, 2022
Version of record online: November 10, 2022